Image Quality Required for the Diagnosis of Skull Fractures Using Head CT: A Comparison of Conventional and Improved Reconstruction Kernels

S. Takagi, M. Koyama, K. Hayashi, and T. Kawauchi

ABSTRACT

BACKGROUND AND PURPOSE: Although skull fractures are generally assessed on bone images obtained by using head CT, the combined multikernel technique that enables evaluation of both brain and bone through a change in the window settings of an image set has been reported. The purpose of this retrospective study was to determine the image quality required for the accurate assessment of skull fractures by using head CT.

MATERIALS AND METHODS: A random sample of 50 patients (25 nonfracture and 25 simple nondisplaced skull fractures) was selected, and sets of conventional brain and bone images and improved combined multikernel images were reconstructed (4614 images). Three radiologists indicated their confidence levels regarding the presence of skull fractures by marking on a continuous scale for each image set. The mean area under the receiver operating characteristic curve was calculated for each kernel, and the statistical significance of differences was tested by using the Dorfman-Berbaum-Metz method.

RESULTS: Although a difference in the diagnostic performance of the 3 radiologists was suggested, the mean area under the curve value showed no significant differences among the 3 reconstruction kernels ($P = .95$ [bone versus combined]), $P = .91$ [bone versus brain]), and $P = .88$ [brain versus combined]). However, the quality of brain images was distinctly poorer than the quality of the other 2 images.

CONCLUSIONS: There was no significant difference in the diagnostic performance of brain, bone, and combined multikernel images for skull fractures. Skull fracture diagnosis is made possible by brain image assessments. Combined multikernel images offer the advantage of high-quality brain and bone images.

ABBREVIATIONS: AUC = area under the receiver operating characteristic curve; ROC = receiver operating characteristic

The quality of CT images reconstructed with conventional filtered back-projection depends on the type of reconstruction kernel used. In head CT, low-pass filter kernels that decrease higher spatial frequencies and noise are generally used to reconstruct brain images, whereas high-pass filter kernels that preserve higher spatial frequencies and increase noise are generally used to reconstruct bone images.[1,2] In all cases, the reconstruction of brain images is required. In contrast, according to the policy of each institution, bone images are reconstructed either in all cases or only for patients with clinically suspected bone disease. Because

assessment of bone tissue is not required for all cases, worthless images increase if there is reconstruction for all cases. However, when bone images are reconstructed only in case of clinical suspicion, additional reconstruction is required if the need for bone images is determined after examination (in the situation of assessing brain images) or if the radiology technician forgets to reconstruct before sending the images (despite reconstruction of bone image being ordered in advance). Furthermore, bone image reconstruction is not possible once the raw data are deleted from the CT device. Although observers have to assess the bone tissue on brain images reconstructed by low-pass filter kernels in such cases, to our knowledge, the diagnostic performance for bone lesions has not been reported.

To resolve this issue, the usefulness of a combined multikernel technique that enables the evaluation of both brain and bone through a change in the window settings of an image set for the assessment of skull fractures has been reported.[3,4] The use of this technique not only decreases the number of stored images and

FIG 1. Images obtained by using bone window settings for a 44-year-old man with a nondisplaced occipital bone fracture. *A*, Bone image. *B*, Brain image. *C*, Combined multikernel image. Though the skull fracture is detectable on all images, the quality of the brain image is distinctly poorer than the quality of the other 2 images. The quality of the combined multikernel image is almost equal to that of the bone image.

AUC values for the different CT reconstruction kernels used for the diagnosis of skull fractures

Observer	Reconstruction Kernel		
	Bone	Brain	Combined
1	0.840	0.853	0.812
2	0.945	0.943	0.915
3	0.946	0.946	0.998
Mean	0.910	0.914	0.908

simplifies head CT examinations, but also enables the assessment of bone tissue in all cases. However, the diagnostic performance of this technique has not been sufficiently investigated.

The purpose of this study was to determine the CT image quality required for the assessment of skull fractures by using receiver operating characteristic (ROC) analysis of different reconstruction kernels and to evaluate the diagnostic performance of the combined multikernel technique for skull fractures.

MATERIALS AND METHODS
Data Base
A random sample of 50 patients (25 nonfracture and 25 simple nondisplaced skull fractures; age, 16–86 years) who visited National Defense Medical College Hospital between 2007 and 2014 was selected for this retrospective study, which was approved by our institutional review board. The requirement for informed consent was waived. All head CT examinations were performed by using a 64-row multidetector CT scanner (Aquilion 64; Toshiba Medical Systems, Tokyo, Japan). The technical protocol was as follows: peak tube voltage, 120 kV; tube current, 300 mA; gantry rotation period, 1.0 seconds; section collimation, 0.5 mm × 64; and pitch factor, 0.64. The image sets were reconstructed with separate reconstruction kernels (brain, FC21; bone, FC30) at the same thickness (5 mm gapless). The field of view for each image set was modified according to individual requirements. Combined multikernel head CT images were generated by combining the brain and bone images by using the threshold method with customized software developed by Microsoft Visual C# (Microsoft, Redmond, Washington).[3] A total of 4614 images (1538 images per kernel type, approximately 31 images per patient) were analyzed.
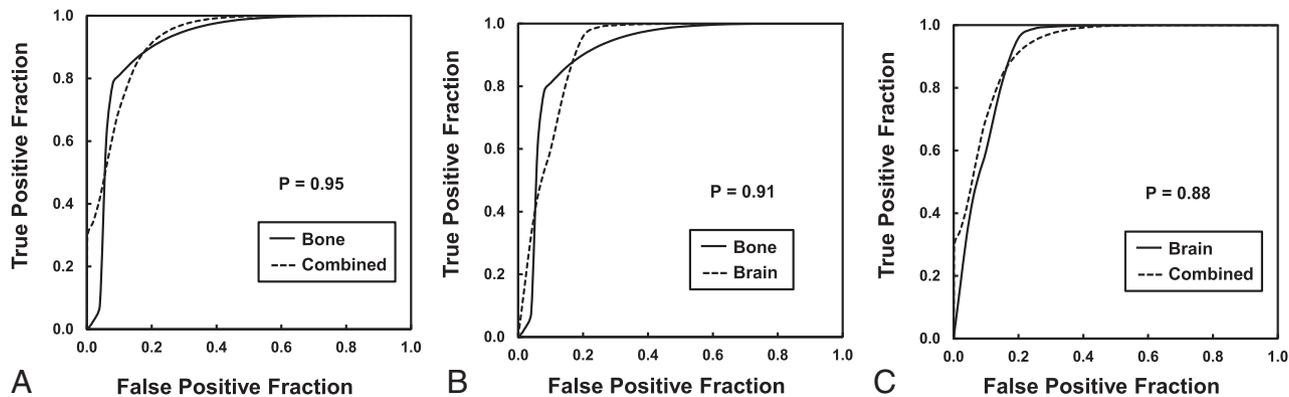
Observer Study
Three radiologists with 10, 15, and 27 years of experience, respectively, independently assessed all patients by using a 3-megapixel, 20.8-inch, monochrome, liquid crystal display monitor. Each type of reconstruction kernel was evaluated once at an interval of more than 4 weeks to prevent learning bias. Images with each type of reconstruction kernel were presented in a random order. The window settings were fixed for all images (window width, 2000 HU; window level, 400 HU). The radiologists indicated their confidence levels regarding the presence of skull fractures by marking on a continuous scale (0–100 on a 100-mm scale, where "0" represented normal and "100" represented definite existence of a skull fracture). No clinical information was provided to the observers.

Statistical Analysis
ROC analysis was used to evaluate the diagnostic performance of the 3 types of reconstruction kernels. Area under the receiver operating characteristic curve (AUC) values were calculated by using ROCKIT software (ROCKIT 0.9B Beta Version, University of Chicago, Chicago, Illinois).[5] The statistical significance of differences in mean AUC values among the 3 reconstruction kernels was tested by using the Dorfman-Berbaum-Metz method, which included both reader variation and case sample variation by an ANOVA approach by using the DBM MRMC software (DBM MRMC 2.1 Beta Version 2 [University of Chicago]).[6,7] A *P* value < .05 was considered statistically significant.

RESULTS
Conventional brain and bone images and a generated combined multikernel image are shown in Fig 1. The AUC values obtained for each observer and each reconstruction kernel are shown in the Table. The mean receiver operating characteristic curves for the 3 observers were generated by PlotROC software (University of Chicago) and are shown in Fig 2 for comparison of the different reconstruction kernels. The skull fracture is clearly seen on the bone and combined multikernel images. Thus, the mean AUC value showed no significant difference between them (*P* = .95). Conversely, although the skull fracture is detectable, the quality of the brain image is distinctly poorer than the quality of the other 2

FIG 2. Comparison of mean ROC curves for the 3 observers for the detection of skull fractures by using 3 different CT reconstruction kernels. *A*, Bone versus combined. *B*, Bone versus brain. *C*, Brain versus combined. There is no significant difference in the mean AUC values among the 3 types of reconstruction kernels.

images. However, the mean AUC value showed no significant difference between the brain image and the bone ($P = .91$) and combined multikernel images ($P = .88$). Therefore, although a difference in AUC values was suggested among the 3 observers, the effect of the type of reconstruction kernel on the diagnostic performance was not statistically significant.

DISCUSSION

We determined the CT image quality required for the assessment of skull fractures by using ROC analysis of different reconstruction kernels and evaluated the diagnostic performance of the combined multikernel technique for skull fractures. Skull fractures are strongly associated with epidural hematoma in patients with acute head injuries.[1,8] Furthermore, the relationship between skull fractures and the development of a delayed epidural hematoma after the evacuation of a contralateral hematoma has also been reported.[9,10] Therefore, misdiagnosis of skull fracture because of poor image quality caused by the use of inadequate reconstruction kernels should be avoided.

Generally, skull fractures must be diagnosed by using bone images.[1,2] However, we observed no significant differences in diagnostic performance among the 3 types of reconstruction kernels used for the assessment of skull fractures in this study. This was an interesting finding, suggesting that the diagnostic performance of head CT for skull fractures does not depend on the image quality, even if images are reconstructed by low-pass filter kernels that decrease higher spatial frequencies. In fact, the skull fracture also could be detected on brain images because of the lower CT value (Fig 1). However, the quality of brain images was distinctly poorer than the quality of bone and combined multikernel images.

Though the quality of combined multikernel images for the diagnosis of skull fractures has been reported to be poorer than the quality of bone images,[3] we observed no significant differences in the present study. The quality of combined multikernel images has also been reported to be clearly better than the quality of brain images when bone window settings are used and equal to the quality of brain images when brain window settings are used.[3] Conversely, the disadvantages of conventional 2D bone images and the efficacy of additional 3D CT image reconstruction have been reported.[2,11] Therefore, we recommend combined multi-

kernel image and 3D image reconstruction for improved diagnostic performance for skull fractures and simplification of head CT examinations.

Recently, the usefulness of full iterative reconstruction techniques with regard to a lower radiation dose and improved image quality has been reported.[12-20] The CT value for each tissue and the window settings in the full iterative reconstruction technique remain unchanged compared with those in the conventional filtered back-projection technique. Model-based iterative reconstruction has no reconstruction parameters.[12,13] Therefore, it enables the evaluation of each tissue through a change in the window settings of an image set and avoids the unnecessary reconstruction of several image sets at each level. However, model-based iterative reconstruction requires more than 30 minutes for the reconstruction process, which is not feasible for emergency cases.[15-17] Conversely, knowledge-based iterative model reconstruction allows rapid reconstruction in less than 5 minutes,[18] which is acceptable in clinical settings. However, because knowledge-based iterative reconstruction requires several reconstruction parameters (image definition and noise reduction),[19,20] there is a requirement of reconstruction of 2 image sets for optimum diagnosis of both the brain parenchyma and the skull. Therefore, we believe that the combined multikernel technique can be applied not only with the conventional filtered back-projection technique, but also with the more recent full iterative reconstruction technique.

This study has some limitations. First, although the types of reconstruction kernels differ among CT device manufacturers, we analyzed only a pair of reconstruction kernels in the present study. However, the diagnostic performance might differ for other pairs of reconstruction kernels in equipment provided by other manufacturers. Second, the evaluation time for each image set was not measured. Although the AUC values were similar, the quality of brain images was poorer than the quality of the other 2 images. Because the type of reconstruction kernel should not burden the observer, further studies should take observer stress caused by image quality into account.

CONCLUSIONS

In this study, there was no significant difference in the diagnostic performance of brain, bone, and combined multikernel images for skull fractures. Therefore, it was revealed that the diagnosis of

skull fracture is made possible by the assessment of brain images. However, the quality of brain images is distinctly poor, and combined multikernel images offer the advantage of high-quality brain and bone images. The combined multikernel technique might be applicable to other reconstruction procedures, such as the more recent full iterative reconstruction technique. Thus, further studies that reveal the usefulness of the combined multikernel technique by comparing other pairs of reconstruction kernels are required for clinical application.

REFERENCES

1. Lolli V, Pezzullo M, Delpierre I, et al. **MDCT imaging of traumatic brain injury.** *Br J Radiol* 2016;89:20150849 CrossRef Medline

2. Dundamadappa SK, Thangasamy S, Resteghini N, et al. **Skull fractures in pediatric patients on computerized tomogram: comparison between routing bone window images and 3D volume-rendered images.** *Emerg Radiol* 2015;22:367–72 CrossRef Medline

3. Takagi S, Nagase H, Hayashi T, et al. **Combined multi-kernel head computed tomography images optimized for depicting both brain parenchyma and bone.** *J Xray Sci Technol* 2014;22:369–76 CrossRef Medline

4. Weiss KL, Cornelius RS, Greeley AL, et al. **Hybrid convolution kernel: optimized CT of the head, neck, and spine.** *AJR Am J Roentgenol* 2011;196:403–06 CrossRef Medline

5. Metz CE, Herman BA, Shen JH. **Maximum likelihood estimation of receiver operating characteristic (ROC) curves from continuously-distributed data.** *Stat Med* 1998;17:1033–53 Medline

6. Dorfman DD, Berbaum KS, Metz CE. **Receiver operating characteristic rating analysis. Generalization to the population of readers and patients with the jackknife method.** *Invest Radiol* 1992;27:723–31 CrossRef Medline

7. Hillis SL, Berbaum KS, Metz CE. **Recent developments in the Dorfman-Berbaum-Metz procedure for multireader ROC study analysis.** *Acad Radiol* 2008;15:647–61 CrossRef Medline

8. Hayashi T, Kameyama M, Imaizumi S, et al. **Acute epidural hematoma of the posterior fossa–cases of acute clinical deterioration.** *Am J Emerg Med* 2007;25:989–95 CrossRef Medline

9. Su TM, Lee TH, Chen WF, et al. **Contralateral acute epidural hematoma after decompressive surgery of acute subdural hematoma: clinical features and outcome.** *J Trauma* 2008;65:1298–302 CrossRef Medline

10. Mohindra S, Mukherjee KK, Gupta R, et al. **Decompressive surgery for acute subdural haematoma leading to contralateral extradural haematoma: a report of two cases and review of literature.** *Br J Neurosurg* 2005;19:490–94 Medline

11. Orman G, Wagner MW, Seeburg D, et al. **Pediatric skull fracture diagnosis: should 3D CT reconstructions be added as routine imaging?** *J Neurosurg Pediatr* 2015;16:426–31 CrossRef Medline

12. Patino M, Fuentes JM, Hayano K, et al. **A quantitative comparison of noise reduction across five commercial (hybrid and model-based) iterative reconstruction techniques: an anthropomorphic phantom study.** *AJR Am J Roentgenol* 2015;204:W176–83 CrossRef Medline

13. Löve A, Olsson ML, Siemund R, et al. **Six iterative reconstruction algorithms in brain CT: a phantom study on image quality at different radiation dose levels.** *Br J Radiol* 2013;86:20130388 CrossRef Medline

14. den Harder AM, Willemink MJ, Budde RP, et al. **Hybrid and model-based iterative reconstruction techniques for pediatric CT.** *AJR Am J Roentgenol* 2015;204:645–53 CrossRef Medline

15. Fontarensky M, Alfidja A, Perignon R, et al. **Reduced radiation dose with model-based iterative reconstruction versus standard dose with adaptive statistical iterative reconstruction in abdominal CT for diagnosis of acute renal colic.** *Radiology* 2015;276:156–66 CrossRef Medline

16. Scott Kriegshauser J, Naidu SG, Paden RG, et al. **Feasibility of ultra-low radiation dose reduction for renal stone CT using model-based iterative reconstruction: prospective pilot study.** *Clin Imaging* 2015;39:99–103 CrossRef Medline

17. Notohamiprodjo S, Deak Z, Meurer F, et al. **Image quality of iterative reconstruction in cranial CT imaging: comparison of model-based iterative reconstruction (MBIR) and adaptive statistical iterative reconstruction (ASiR).** *Eur Radiol* 2015;25:140–46 CrossRef Medline

18. Mehta D, Thompson R, Morton T, et al. **Iterative model reconstruction: simultaneously lowered computed tomography radiation dose and improved image quality.** *Med Phys Int* 2013;1:147–55

19. Nakaura T, Iyama Y, Kidoh M, et al. **Comparison of iterative model, hybrid iterative, and filtered back projection reconstruction techniques in low-dose brain CT: impact of thin-slice imaging.** *Neuroradiology* 2016;58:245–51 CrossRef Medline

20. Suzuki S, Haruyama T, Morita H, et al. **Initial performance evaluation of iterative model reconstruction in abdominal computed tomography.** *J Comput Assist Tomogr* 2014;38:408–14 CrossRef Medline